Pertanika J. Sci. & Technol. 34 (2): 1163 - 1180 (2026)

PERTANIKA JOURNALS

SCIENCE & TECHNOLOGY

Journal homepage: http://www.pertanika.upm.edu.my/

Quantification of Some Physical Properties of Matoa (*Pometia pinnata*) Fruit: Mass Modelling for Machine Designing and Postharvest Processing

Ubaidillah Ubaidillah*, Risty Dwi Wulandari Silalahi, Dimas Firmanda Al Riza, and Bambang Dwi Argo

Department of Biosystems Engineering, Faculty of Agricultural Technology, Universitas Brawijaya, 65145 East Java, Indonesia

ABSTRACT

Matoa (*Pometia pinnata*) is an underutilised seasonal fruit commonly consumed raw in Indonesia. Despite its nutritional, health, and economic benefits, it lacks postharvest processing and derivative products. This study quantified the physical and thermal properties of matoa fruit to aid in the design of processing equipment. The fruit's principal dimensions averaged 39.30±3.19 mm in length, 29.35±1.41 mm in width, and 28.72±1.38 mm in thickness. The mass ranged from 6.51 to 21.31 g, with volumes between 10.5 and 24.5 cm^3. The average geometric and equivalent diameters were 32.10 mm, and the fruit had an ellipsoid shape. The static coefficient of friction was highest on galvanised iron and lowest on stainless steel. Four empirical models, i.e. linear, quadratic, power, and S-curve, were evaluated to predict fruit mass using physical attributes. The multivariate quadratic model with principal dimensions (*LWT*) provided the highest R^2 value for mass prediction. These findings offer a scientific basis for designing grading, sorting, and processing equipment, and for developing postharvest and derivative products.

Keywords: Mathematical modelling, matoa fruit, postharvest handling, regression, underutilised fruit

ARTICLE INFO

Article history:
Received: 16 November 2025
Accepted: 24 December 2025
Published: 30 April 2026

DOI: https://doi.org/10.47836/pjst.34.2.23

E-mail addresses:
ubaidillah88@ub.ac.id (Ubaidillah Ubaidillah)
ristysilalahi567@gmail.com (Risty Dwi Wulandari Silalahi)
dimasfirmanda@ub.ac.id (Dimas Firmanda Al Riza)
dwiargo@ub.ac.id (Bambang Dwi Argo)
* Corresponding author

INTRODUCTION

Pometia pinnata is an underutilised tropical fruit tree in the *Sapindaceae* family, and popular as Fijian longan in English or matoa in Indonesia (Matra et al., 2019). The study of the variability of the genus Pometia in Indonesia, including *Pometia pinnata*, has been reported as early as the 1960s (Jacobs, 1962). The species is distributed throughout

e-ISSN: 2231-8526

its origins across tropical Asia and the Asia Pacific region, including areas such as the Andaman Islands, Sri Lanka, Southeast Asia, and Papua New Guinea. In Java, matoa is rarely grown in dedicated orchards and typically maintained as a backyard crop. Matoa is considered a seasonal fruit, with a flowering season from around July to October and harvest season from around October to December. The fleshy fruit is edible, and it has been extensively reported for its health benefits (Suzuki et al., 2021). Its by-products also have potential bioactivities but are inedible, including seeds, rind, stem bark and leaves (Hanafi et al., 2020). The matoa tree is also widely used as timber for housing (Burley et al., 2011) and is also planted for aesthetic and functional purposes, such as fencing, marking boundaries, or providing shade.

Although the nutrient composition of the edible fruit has not been published previously (Lim, 2013), there has been research on the medicinal utilisation of matoa fruit. All the fruit parts, i.e., rind, edible arillode, and seed, have total phenolic content including n-hexane, ethyl acetate and methanol as reported previously by Irawan et al. (2017a). Irawan et al. (2017b) also evaluated the DPPH free radical scavenging activity of all fruit parts. The matoa fruit has a generally rounded to oval-elliptic form. It has a smooth rind that ranges from thin to moderately thick, displaying colour variations from yellow-green to deep red or nearly black. The rind encloses an edible gelatinous, juicy, sweet, semi-transparent white, pulpy arillode that envelops a single large, curved seed. The arillode is traditionally eaten raw, with no further processing or derivative products available on the market. The problem with seasonal fruits in Indonesia, especially matoa, is that the fruits are abundantly available in the market for a certain limited time window, with a low consumption rate due to being eaten raw. As a result, the fruit may end up as food waste during the harvest season. The fruit is considered an underutilised fruit attributed to its highly perishable character, lack of processing knowledge and derivative products, despite its nutritional and health benefits as well as economic potential. To increase its potential and benefits, further processing and derivative product development are mandatory.

Well-developed postharvest processing and its machines are urgently needed to enhance and commercialise the utilisation of matoa fruit. The physical and thermal properties and their interactions with the fruit materials must be well understood to enable the design and optimisation of processing machinery (Kamble et al., 2021). The absence of physical and thermal attributes may increase product losses, product failure, and mechanical breakdown. The appropriate processing and machinery design can result in increased work efficiency and adequate process applications (Vivek et al., 2018). The comprehensive quantifications and understanding of the engineering characteristics of matoa fruit give substantial input for researchers, machine designers, and food-product developers (Murakonda et al., 2022). Various basic processing and handling, including peeling, cutting, grading, separation, cleaning, conveying, packaging, transportation, and other postharvest tools,

are fundamentally influenced by fruit physical properties, e.g., size, mass, volume, density, shape, surface area, porosity, appearance, fraction of fruit parts, as well as fruit frictional properties (Barbhuiya et al., 2020). In addition, quantification of the thermal characteristics, namely heat conductivity, specific heat, diffusivity, and latent heat, can help in various thermal processing and preservation activities involving heat transfer, such as cooking, drying, refrigeration, thermal treatment, and freezing operations (Singh et al., 2019; Singh & Meghwal, 2019). The design of the effective storage and cooling systems for the fruit also needs to consider the usefulness of the thermal properties (Sonawane et al., 2020).

In recent years, the market acceptability of the fruit has been mainly influenced by specific traits, i.e., similar size and weight and uniform shape. Mass-based fruit grading is beneficial for packaging since it can improve packaging formations and configurations, reduce handling waste and transport resources, and develop the marketability of the fruit (Birania et al., 2022). Mass-based fruit grading is also simpler and cheaper to conduct than grading based on other attributes, i.e., by either using direct weighing or applying appropriate empirical models that can predict the fruit mass from measurable physical parameters (Mahawar et al., 2019). Since direct weighing is time-consuming and tedious, it seems plausible to develop an appropriate mathematical model to estimate the matoa fruit mass based on physical attributes. The developed fruit mass models could provide a rapid, precise, simple, and cheap fruit classification and grading process.

Numerous investigations have been conducted in the past few years for the development of an appropriate mathematical model for estimating the mass of agricultural commodities using their measurable physical parameters. These investigations encompass an array of agricultural products, spanning both underutilised and widely recognised commodities. Noteworthy examples include sohiong fruit (Vivek et al., 2018), *Terminalia chebula* and *Terminalia bellerica* fruit (Pathak et al., 2019; Pathak et al., 2020), kinnow mandarin (Mahawar et al., 2019), pepper berries (Azman et al., 2020), ash gourd seed (Gade et al., 2020), Indian coffee plum (Barbhuiya et al., 2020), kendu fruit (Panda et al., 2020), green plantain banana (Kamble et al., 2021), blood fruit (Sasikumar et al., 2021), hempseed (Saini et al., 2021), strawberry (Birania et al., 2022), wood apple (Murakonda et al., 2022), kadamb (Panda et al., 2022), amla (Tomar & Pradhan, 2022), guava (Bibwe et al., 2022), and potato (Altuntas & Mahawar, 2022).

Despite the phenotype variability of the fruit being previously reported (Zulfahmi & Rosmaina, 2024), to our knowledge, no prior publication has addressed the physical and thermal characteristics of matoa fruit. Hence, the objective of the present study was to quantify in detail various key physical and thermophysical parameters of matoa fruit that are needed for proper machine design and postharvest processing. In addition, to establish a mathematical model that appropriately correlates the primary physical variables and fruit mass of the matoa fruit. The commonly used four regression forms-linear, quadratic,

power, and S-curve-were applied for estimating the fruit mass. The findings of the present research are expected to promote enhanced utilisation and market development of matoa, thereby supporting the economic well-being of local farmers.

METHODS

Sample Preparation

Fresh and mature matoa fruits (Figure 1) were procured during the harvesting season (October 2023), sourced from smallholder orchards in Wates Village (7°55′ S, 112°7′ E), Kediri Regency, East Java, Indonesia. The collected fruits were transported promptly to the Department of Biosystems Engineering, Universitas Brawijaya, for further analysis. After manual removal of peduncles, leaves, and dust, the fruits were sorted by eliminating defective, broken, and bruised fruits and stored at ambient temperature until further experiments. The measurements were conducted in less than 24 h after harvest. The experiments on physical and thermal properties were conducted in the Laboratory of Agricultural Power and Machinery, Universitas Brawijaya. In total, 200 samples were randomly selected for physical and thermal properties quantification, i.e., 183 samples for physical properties and the remaining for thermal properties.

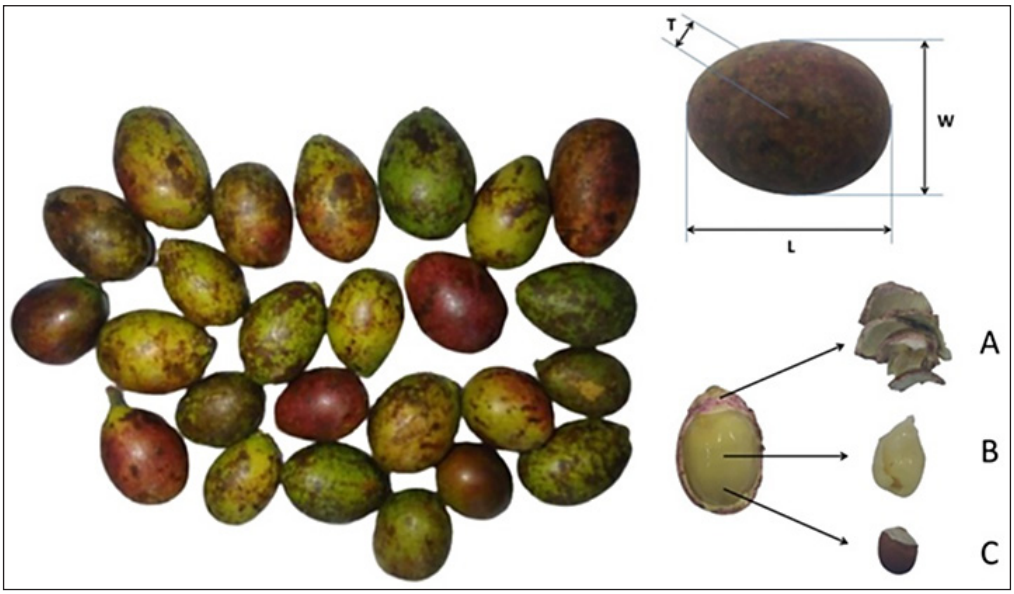

Figure 1. Representation of collection and measuring principal dimension of matoa (Pometia pinnata) fruit: (A) rind; (B) edible arillode; and (C) seed

Quantification of Physical Properties

Dimensional Properties of the Matoa Fruit

The 183 fruits were selected at random from the bulk sample to determine the physical characteristics of matoa. The dimensional properties, i.e., axial dimension, mass, and volume of each matoa fruit, were measured manually. The principal dimensions of the fruit, namely length (L), width (W), and thickness (T), as illustrated in Figure 1, are measured using a digital vernier calliper with ±0.01 mm accuracy (Mitutoyo, Japan). The mass of each fruit (M) was measured using a digital balance with ±0.001 g accuracy (FSR-A320, Fujitsu, Japan). The volume of each individual fruit was measured by employing the water displacement method (Mahawar et al., 2019; Vivek et al., 2018). Table 1 shows the equations used for the quantification of physical properties of matoa fruits.

Gravimetric Properties

The cardboard container with certain dimensions (235×175×70) mm^3 was utilised to determine the matoa fruit bulk density sample, and calculated using the following equation (Panda et al., 2020), where ρ_B, m_{c+f}, m_c, and V_c represent bulk density of fruit, mass of container with fruit, mass of container, and volume of container, respectively as shown in Equation 1.

$$\rho_B = \frac{m_{c+f} - m_c}{V_c} \quad [1]$$

The true density (ρ_T) was calculated using Equation 2, which represents the ratio of a unit mass of each fruit (M) to its true volume (V_t) (Pathak et al., 2019).

$$\rho_T = \frac{M}{V_t} \quad [2]$$

The porosity or void fraction is defined as the ratio of inter-granular voids to the total space occupied by the fruit, and calculated using Equation 3, where ε, ρ_B, and ρ_T represent porosity, bulk density, and true density, respectively (Barbhuiya et al., 2020).

$$\varepsilon = \frac{\rho_T - \rho_B}{\rho_T} \times 100 \quad [3]$$

Table 1
Equations for the physical properties of the matoa fruits

Attributes	Equation
Arithmetic mean diameter (D_a)	$D_a = \frac{(L+W+T)}{3}$
Geometric mean diameter (D_g)	$D_g = (L \times W \times T)^{\frac{1}{3}}$
Equivalent mean diameter (D_e)	$D_e = \left(\frac{\left\{ L \times (W+T)^2 \right\}}{4} \right)^{\frac{1}{3}}$
Surface area (SA)	$SA = \pi \left(D_g \right)^2$
Projected area perpendicular to length (PA_L)	$PA_L = \frac{\pi LW}{4}$
Projected area perpendicular to width (PA_W)	$PA_W = \frac{\pi WW}{4}$
Projected area perpendicular to thickness (PA_T)	$PA_T = \frac{\pi TW}{4}$
Criteria projected area (CPA)	$CPA = \frac{PA_L + PA_W + PA_T}{3}$
Sphericity (Ø)	$A_R = \frac{W}{L}$
Aspect ratio (A_R)	$A_R = \frac{W}{L}$
Flakiness ratio (F_R)	$E_R = \frac{L}{W}$
Elongation ratio (E_R)	$E_R = \frac{L}{W}$
Eccentricity (e)	$e = \left[1 - \left(\frac{W}{L} \right)^2 \right]^{\frac{1}{2}}$

Table 1 (*continued*)

Attributes	Equation
Minimum radius curvature (R_{min})	$R_{\min} = \frac{H}{2}$
Maximum radius curvature (R_{max})	$R_{\max} = \frac{H^2 + \frac{L^2}{4}}{2 \times H}$
Ellipsoid volume (V_{ellip})	$V_{ellip} = \frac{4\pi}{3} \times \left(\frac{L}{2}\right) \times \left(\frac{W}{2}\right) \times \left(\frac{T}{2}\right)$
Oblate spheroid volume (V_{osp})	$V_{osp} = \frac{4\pi}{3} \times \left(\frac{L}{2}\right) \times \left(\frac{W}{2}\right)^2$
Prolate spheroid volume (V_{pro})	$V_{pro} = \frac{4\pi}{3} \times \left(\frac{L}{2}\right)^2 \times \left(\frac{W}{2}\right)$

Note. Adapted from Sahin and Sumnu (2007) and Thomas et al. (2025)

Frictional Properties

The static friction coefficient of matoa fruit was measured using a friction testing apparatus employing five surface materials, i.e., plywood, galvanised iron sheet, stainless steel sheet, rubber sheet, and cardboard. The materials were chosen since they are the most common materials used for machinery, transportation, and packaging. The measurements of the static coefficient of friction were made in two orientations, i.e., along the fruit's longitudinal axis and across its radial directions from the calyx end. Each fruit was placed on the surface material, and the platform was slowly inclined until the fruit began to move and eventually slide or roll off. The static coefficient of friction for matoa fruit is then calculated using Equation 4 as follows, where μ and α represent the static coefficient of friction and the angle of friction or inclination angle at which the fruit starts to roll or fall (°) (Panda et al., 2020).

$$\mu = \tan\alpha \quad [4]$$

Fruit Part Fraction Determination

The fruit fraction was determined to estimate the portion of the rind, arillode, and seed for one individual matoa fruit. Each fruit was manually peeled by hand and separated for

each fruit part, i.e., rind, arillode, and seed (Figure 1). The masses of the rind, arillode, and seed for each fruit were recorded using a digital balance, and their proportions relative to the whole-fruit mass were calculated.

Quantification of Thermal Properties

The four primary thermal properties of matoa, namely specific heat capacity (*Cp*), thermal conductivity (*K*), thermal diffusivity (μ), and latent heat (λ), were estimated using the moisture content of the edible arillode. The moisture content of the edible arillode of matoa fruit was determined using a hot-air oven at 105±5°C for 24 h according to (Association of Official Analytical Chemists, 2000). Since the moisture content (m) of the arillode is higher than 60%, the standard mathematical formulas as in Equations 5-8 proposed by Sweat (1974) were used, where Cp, K, μ, λ, ρ_T, W, and m represent specific heat capacity, thermal conductivity, thermal diffusivity, latent heat of fusion, true density, weight, and moisture content.

$$Cp = 1.675 + 0.025m \quad [5]$$

$$K = 0.148 + 0.00493m \quad [6]$$

$$\mu = \frac{K}{\rho_T Cp} \quad [7]$$

$$\lambda = 335W \quad [8]$$

Mass Modelling of the Matoa Fruit

The non-linear regression analysis of data from the physical properties of matoa fruit was done using the Microsoft Excel 2010. The four most commonly used models to predict the mass of agricultural products Equations 9 to 12, i.e., linear, quadratic, power, and S-curve, were applied to analyse their suitability for mass prediction of matoa fruit, where M is the mass of the fruit, X is the considered physical parameter utilised for evaluating the relationship with mass, and a, b, and c are the constants of curve fitting (Saini et al., 2022).

$$M = a + bX \quad [9]$$

$$M = a + bX + cX^2 \quad [10]$$

$$M = a(X)^b \quad [11]$$

$$M = a + \left(\frac{b}{X}\right) \quad [12]$$

The mass data of matoa fruit was modelled using independent variables from the physical attributes of the matoa fruit, namely dimensional properties, area, and volume (Kamble et al., 2021), and the whole model was classified as follows:

1. Dimension-based models: single or multiple variable regression of dimensional attributes of matoa fruit: *L*, *W*, *T*, *Da*, *Dg*, and *De*;
2. Area-based models: single variable regression of area attributes of matoa fruit: *SA*, PA_L, PA_W, PA_T, and *CPA*;
3. Volume-based models: single variable regression of volume attributes of matoa fruit: *V*, V_{ellip}, V_{osp}, and V_{pro}.

Statistical Analysis and Model Validation

Descriptive statistics (mean, minimum, maximum, and standard deviation) for all measured physical and thermal attributes of the fruit were calculated using the Microsoft Excel 2024 software. The applied model's performance was tested using three statistical indicators, i.e., the coefficient of determination (R^2), root-mean-square error (*RMSE*), and reduced chi-square (χ^2) between actual and predicted mass values. These indicators were used to identify the most suitable model, with R2 serving as primary selection criterion, whereas RMSE and χ^2 were used to evaluate the model's goodness of fit. The regression model which has the higher coefficient of determination (R^2) and lower root-mean-square error (*RMSE*) as well as reduced mean square of deviation (χ^2) were selected as the best fit (Saini et al., 2022). RMSE and χ^2 were computed using Equations 13 and 14, respectively, where $M_{ex,i}$ denotes the *i*-th measured mass, $M_{pr,i}$ represents the *i*-th predicted mass, *N* is the total number of samples, and *z* is the number of model parameters

$$RMSE = \left[\frac{1}{N}\sum_{i=1}^{N}\left(M_{pr,i} - M_{ex,i}\right)^2\right]^{1/2} \quad [13]$$

$$\chi^2 = \frac{\sum_{i=1}^{N}\left(M_{ex,i} - M_{pr,i}\right)^2}{N - z} \quad [14]$$

RESULTS AND DISCUSSION

Physical Properties

The dimensional characteristics of whole matoa fruits were evaluated at a natural moisture content of 37.55±2.75% (w.b.), and the corresponding mean values with standard deviations

are summarised in Table 2. Based on the measurement results, the mean values for fruit length (*L*), width (*W*), and thickness (*T*) were 39.30±3.19 mm, 29.35±1.41 mm, and 28.72±1.38 mm, respectively. The dimensions of matoa fruit are relatively bigger than both dimensions of the fruit with similar shapes, i.e., *Haematocarpus validus* and *Prunus nepalensis* L (Sasikumar et al., 2021; Vivek et al., 2018). The average mass (*M*) of the whole matoa fruit is 15.31±2.44 g, and the average consumable portion available in the fruit, i.e., arillode, is 57.13±4.35%, while the rest is a non-consumable portion in the form of rind and seed.

Table 2
Physical parameters

No.	Physical Properties	N	Mean	Min	Max	SD
1	Mass *M* (g)	183	15.31	6.51	21.31	2.44
2	Length *L* (mm)	183	39.30	27.30	50.20	3.19
3	Width *W* (mm)	183	29.35	24.90	32.60	1.41
4	Thickness *T* (mm)	183	28.72	24.40	31.70	1.38
5	Arithmetic mean diameter D_a (mm)	183	32.46	27.57	37.30	1.78
6	Geometric mean diameter D_g (mm)	183	32.10	27.48	36.29	1.69
7	Equivalent mean diameter D_e (mm)	183	32.10	27.48	36.29	1.69
8	Projected area perpendicular to length *PA-L* (mm^2)	183	908.03	602.50	1226.18	105.95
9	Projected area perpendicular to width *PA-W* (mm^2)	183	678.01	486.95	834.69	64.54
10	Projected area perpendicular to thickness *PA-T* (mm^2)	183	663.48	479.13	811.65	62.19
11	Criteria projected area *CPA* (mm^2)	183	749.84	543.67	911.09	74.12
12	Surface area (mm^2)	183	3246.29	2371.63	4136.25	339.35
13	Aspect ratio (decimal)	183	0.75	0.61	0.90	0.05
14	Sphericity (decimal)	183	0.82	0.71	0.92	0.03
15	Eccentricity (decimal)	183	0.66	0.44	0.79	0.05
16	Radius of curvature minimum R_{min} (mm)	183	17.16	13.85	20.33	1.05
17	Radius of curvature maximum R_{max} (mm)	183	22.79	17.21	28.07	1.61
18	Elongation ratio (decimal)	183	1.34	1.11	1.64	0.08
19	Flakiness ratio (decimal)	183	0.98	0.88	0.99	0.02
20	True volume (mm^3)	183	17628.42	10500	24500	2751.85
21	Ellipsoid volume (mm^3)	183	17463.31	10860.33	25014.06	2720.40
22	Prolate spheroid volume (mm^3)	183	24003.30	10965.55	41036.13	4691.35
23	Oblate spheroid volume (mm^3)	183	17848.64	11037.64	25422.78	2817.40
24	True density (g/cm^3)	183	0.87	0.48	1.22	0.08
25	Bulk density (g/cm^3)	-	0.54	0.53	0.55	0.02
26	Porosity (%)	-	37.90	36.45	39.36	2.05

Table 2 (*continued*)

No.	Physical Properties	N	Mean	Min	Max	SD
27	Fruit part fraction: rind (%)	183	22.30	12.30	52.17	6.27
28	Fruit part fraction: arillode (%)	183	57.13	39.13	68.95	4.35
29	Fruit part fraction: seed (%)	183	20.58	1.83	33.76	4.75
30	Rind thickness (mm)	60	1.43	0.55	3.15	0.52
31	Coefficient of friction					
	Plywood (axial)	30	0.318	0.158	0.488	0.085
	Plywood (radial)	30	0.104	0.070	0.141	0.023
	Galvanized iron sheet (axial)	30	0.348	0.141	0.625	0.110
	Galvanized iron sheet (radial)	30	0.118	0.052	0.194	0.038
	Stainless steel sheet (axial)	30	0.253	0.123	0.554	0.093
	Stainless steel sheet (radial)	30	0.083	0.052	0.141	0.024
	Rubber sheet (axial)	30	0.304	0.087	0.466	0.093
	Rubber sheet (radial)	30	0.087	0.052	0.123	0.022
	Cardboard (axial)	30	0.272	0.158	0.424	0.085
	Cardboard (radial)	30	0.107	0.052	0.213	0.041

A clear representation of the distribution of length (L), width (W), thickness (T), mass (M), and true volume (V) of matoa fruit is depicted in Figure 2. According to Figure 2, the range of approximately 38-41 mm of fruit length is the most frequent length range for matoa fruit (41%). The fruit length also exhibits the highest peak frequency, suggesting that matoa fruits are more uniform in length compared to other parameters. The most frequent width (75%) and thickness (73%) of matoa fruit are falls between approximately 18-31 mm, showing a more symmetrical and narrow distribution compared to length. This alignment of Figure 2 implies that the fruit's mass correlates closely with its volume, reflecting that matoa have a consistent density across the samples. All parameters demonstrate a bell-shaped distribution, with most samples clustering around the central ranges, reflecting natural variability in matoa fruit, which is common in agricultural products.

The mean values for D_a, D_g, and D_e were 32.46±1.78 mm, 32.10±1.69 mm, and 32.10±1.69 mm, respectively. The mentioned average diameters are the basic data needed to determine the aperture size of the machine for segregation and grading based on the dimensions of the fruit (Pathak et al., 2019). The average area parameters of the fruit, namely SA, PA_L, PA_W, PA_T, and CPA, were found to be 3246.29±339.35 mm^2, 908.03±105.95 mm^2, 678.01±64.54 mm^2, 663.48±62.19 mm^2, and 749.84±74.12 mm^2. All mentioned area parameters of the fruit are beneficial in designing sizing systems, dryers and drying systems, storage systems, various aspects of postharvest, and processing of the fruit (Pathak et al., 2019; Pathak et al., 2020).

The shape of the matoa fruit was depicted with its sphericity ($Ø$), aspect ratio (A_R), flakiness ratio (F_R), elongation ratio (E_R), and eccentricity (e) observed as 0.82±0.03,

0.75±0.05, 0.98±0.02, 1.34±0.08, and 0.66±0.05, respectively. According to the obtained data, it indicates that the shape of the fruit seems to exhibit a shape that is closer to an ellipsoid than a perfect sphere due to the higher value of the elongation ratio (E_R). The sphericity ($\varnothing$) and aspect ratio (A_R) of the fruit are responsible for the flow behaviour of the materials, i.e., the higher the sphericity ($\varnothing$), the higher the flowability of the fruit. The flakiness ratio (F_R) and elongation ratio (E_R) of the matoa fruit indicate that the shape of the fruit is not flaked and slightly elongated. All the mentioned shape properties of the matoa fruit indicate that the matoa fruit will roll on the specific test surface and will be a major consideration for designing hoppers. The rolling ability can also be estimated by using the radius of curvature of the matoa fruit, which is very critical for designing conveyors and chutes, i.e., 17.16±1.05 mm of R_{min} and 22.79±1.61 mm of R_{max} for matoa fruit (Pathak et al., 2019; Pathak et al., 2020).

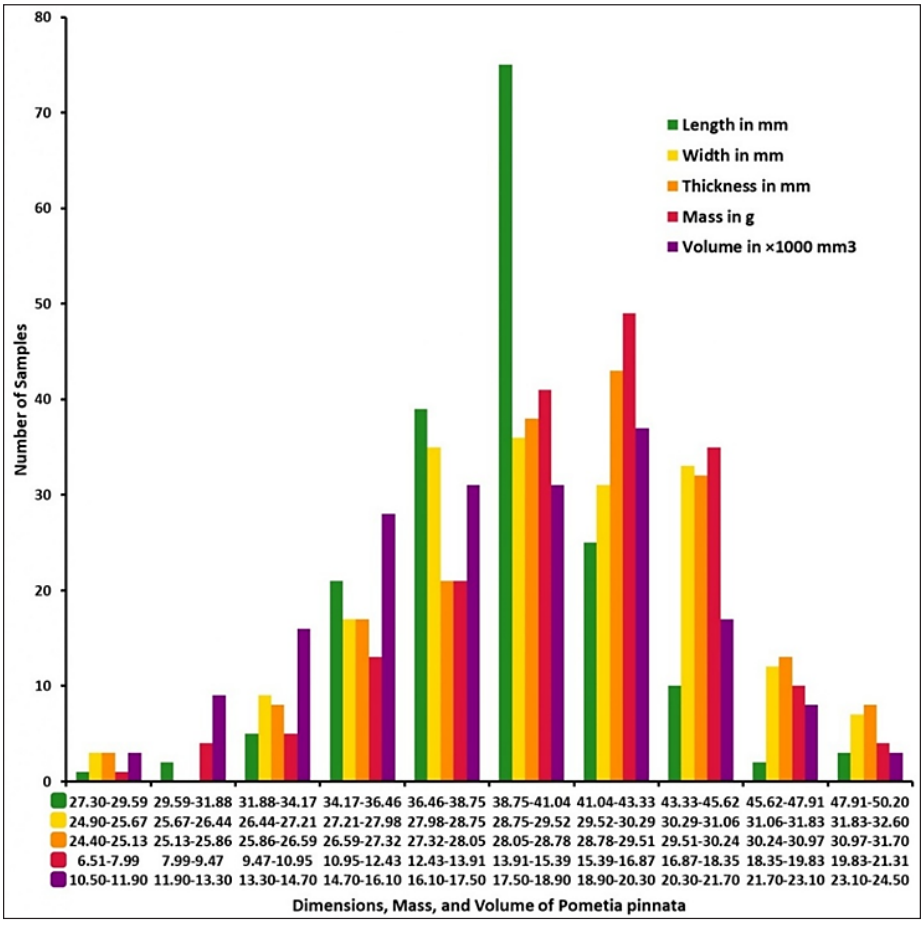

Figure 2. Distribution of length, width, thickness, mass, and true volume

The average volumes for matoa fruit, namely true volume (V), ellipsoid volume (V_{ellip}), prolate spheroid volume (V_{pro}), and oblate spheroid volume (V_{osp}), were recorded as 17628.42±2751.85 mm^3, 17463.31±2720.40 mm^3, 24003.30±4691.35 mm^3, and 17848.64±2817.40 mm^3, respectively. The volume parameters of the fruit are the main factors in calculating the density parameters of the fruit, i.e., bulk density (ρ_B), true density (ρ_T), and porosity (ε). The respective values of average bulk density (ρ_B), true density (ρ_T), and porosity or void fraction (ε) was 0.54±0.02 g/cm3, 0.87±0.08 g/cm3, and 37.90±2.05%. Both volume and density parameters are crucial for designing storage systems such as bins, silos, and storage rooms (Pathak et al., 2019). Both are also very critical inputs to designing efficient packaging, e.g., packaging materials, packaging size, packaging formation, and packaging configuration (Birania et al., 2022; Mahawar et al., 2019). In addition, the volume and density parameters are critical to ensuring the optimum transportation system of the fruit (Sasikumar et al., 2021).

The results also showed that for all tested surfaces, the static friction in the axial orientation was consistently higher than that in the radial orientation. Similar phenomena have been reported previously on Kendu fruit (*Diospyros melanoxylon* Roxb.) (Panda et al., 2020). The obtained average values in the axial direction of the coefficient of friction, from largest to smallest, were galvanised iron sheet, plywood, rubber sheet, cardboard, and stainless-steel sheet, while the coefficient of friction in the radial direction was galvanised iron sheet, cardboard, plywood, rubber sheet, and stainless-steel sheet. The friction coefficients obtained serve as important reference data for the design of conveyors, storage bins, and hopper systems. Similarly, various material handling tools and equipment designs, e.g., chutes and conveyor belts, are completely dependent on the angle of friction to specify their angle of inclination (Vivek et al., 2018).

Thermal Properties

The thermal characteristics of the edible arillode of matoa fruit are summarised in Table 3. The thermal properties of the edible arillode of matoa fruit, namely specific heat capacity (Cp), thermal conductivity (K), thermal diffusivity (μ), and latent heat (λ), were relatively high thanks to the high moisture content, i.e., 73.47±2.50% (w.b.). Thermal properties are beneficial data in food processing and storage, such as fruits, when the contained water in the product is highly responsible (Sasikumar et al., 2021). The thermal conductivity of the edible part of matoa fruit was relatively low (0.51 J/ms °C). This suggests that the edible material has a relatively low capacity to conduct heat, which is important when estimating heat flux during thermal processing. The thermal diffusivity of the arillode was relatively high (1.67×10^{-4} m^2/s), likely due to its high moisture content, which enables heat to move rapidly through the material relative to its bulk capacity. The obtained thermal properties of edible arillode of matoa fruit, i.e., specific heat capacity (Cp), thermal conductivity (K), and

Table 3
Thermal properties

No.	Physical Properties	N	Mean	Min	Max	SD
1	Specific heat capacity *Cp* (kJ/kg °C)	17	3.512	3.456	3.617	0.063
2	Thermal conductivity *K* (J/ms °C)	17	0.510	0.499	0.531	0.012
3	Thermal diffusivity μ ($\times 10^{-4}$ m^2/s)	17	1.670	1.660	1.687	0.010
4	Latent heat of fusion λ (kJ/kg)	17	2.461	2.067	2.832	0.329

thermal diffusivity (μ), were relatively on par with previous reports of fruits, e.g. sohiong fruit (Vivek et al., 2018), cashew apple fruit (Singh et al., 2019), bael fruit (Sonawane et al., 2020), green plantain (Kamble et al., 2021), blood fruit (Sasikumar et al., 2021), and wood apple (Murakonda et al., 2022).

Mass Modelling of the Matoa Fruit

The mathematical models developed to estimate the mass of matoa fruit were analysed based on its dimensions, surface area, and volume. A total of 76 predictive models were evaluated for estimating the mass of matoa fruit, i.e., 40 models for dimensions-based, 20 models for surface area-based, and 16 models for volume-based. The model considered the most suitable when resulting in the highest R^2, as well as the lowest *RMSE* and χ^2. The results showed that the range of R^2 values ranged from 0.423 to 0.915, from 0.668 to 0.843, and from 0.536 to 0.838 for dimension, surface area, and volume-based models, respectively. Table 4 presents the ten best-performing models, which achieved the highest R^2 and the lowest *RMSE* and χ^2 values.

According to Table 4, the dimension-based models are superior to surface area and volume-based models. Based on dimensional properties, the quadratic model Equation

Table 4
The selected ten models with the highest R^2 and the lowest RMSE and χ^2 values

Model-based	Dependent	Independent	Variables	Model	R^2	RMSE	χ^2
Dimension	M	L, W, T	Multivariate	Quadratic	0.915	0.610	0.400
Dimension	M	L, W	Multivariate	Quadratic	0.899	0.660	0.460
Dimension	M	L, W, T	Multivariate	S-curve	0.857	0.790	0.640
Dimension	M	L, W	Multivariate	S-curve	0.852	0.800	0.660
Dimension	M	W, T	Multivariate	Quadratic	0.850	0.810	0.680
Area	M	CPA	Univariate	Quadratic	0.843	0.830	0.700
Dimension	M	L, W, T	Multivariate	Linear	0.842	0.830	0.710
Dimension	M	L, W	Multivariate	Linear	0.838	0.840	0.720
Volume	M	V_{osp}	Univariate	Quadratic	0.838	0.840	0.720
Dimension	M	L, W, T	Multivariate	Power	0.836	0.850	0.730

15 with multiple variables of length (L), width (W), and thickness (T) resulted in the best fit, with 0.915, 0.610, and 0.400 of R^2, *RMSE*, and χ^2 values, respectively. The quadratic model also gives the best fit for the surface area and volume-based models, with the criteria projected area (*CPA*) and volume of the oblate spheroid (V_{osp}) as single independent variables, respectively. The surface area-based model Equation 16 and volume-based model Equation 17 have 0.843 and 0.836, 0.830 and 0.850, and 0.700 and 0.730 for their respective R^2, *RMSE*, and χ^2 values. The selected mass models for matoa fruit based on its dimension, surface area, and volume are shown in Figure 3.

$$M = -84.3474 + 0.1897T + 4.0146W + 0.8720L + 0.0667TL \\ -0.5194TW + 0.0184WT + 0.2116T^2 + 0.1984W^2 - 0.0399L^2 \Rightarrow R^2 = 0.915 \quad [15]$$

$$M = -40.2497 + 0.1217CPA - 6.2726 \times 10^{-5} CPA^2 \Rightarrow R^2 = 0.843 \quad [16]$$

$$M = -17.9169 + 0.0030V_{osp} - 6.4349 \times 10^{-8} V_{osp}^2 \Rightarrow R^2 = 0.838 \quad [17]$$

The previous reports for relatively similar shapes of matoa, i.e., *Haematocarpus validus* and *Prunus nepalensis* L, also indicated the superiority of the quadratic model. For the majority of the mass group of sohiong fruit (*Prunus nepalensis* L), Vivek et al. (2018) recommended the quadratic model for dimension, area, and volume-based model, with length (L) ($R^2 = 0.920$), projected area perpendicular to length (PA_L) ($R^2 = 0.946$), and ellipsoid volume (V_{ellip}) ($R^2 = 0.945$) as independent variables, respectively. Sasikumar et al. (2021) reported that the mass of blood fruit (*Haematocarpus validus*) can be suitably

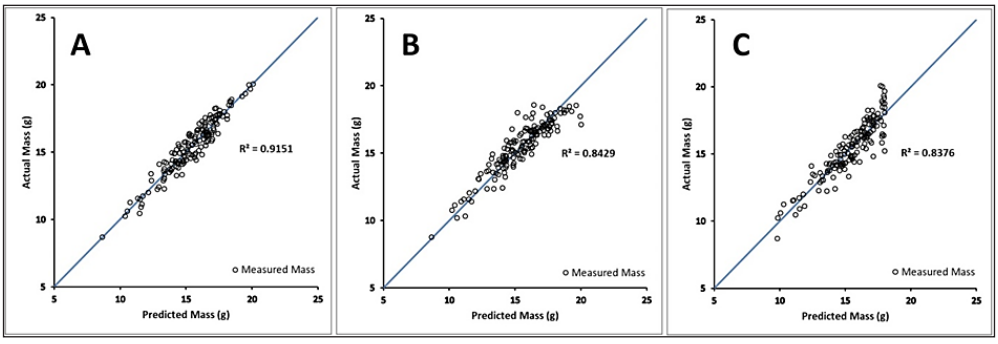

Figure 3. Matoa fruit mass model based on (A) '*LWT*' dimensions; (B) criteria projected area; and (C) volume of an oblate spheroid

predicted using its width (*W*) for dimension-based models in quadratic form ($R^2 = 0.984$), as well as using its criteria projected area (*CPA*) for area-based models in the same form of equation ($R^2 = 0.974$). However, for volume-based models, the linear model was recommended with ellipsoid volume (V_{ellip}) as an independent variable ($R^2 = 0.953$).

CONCLUSION

This study comprehensively quantified the engineering properties of matoa fruit to support the design of appropriate machinery and postharvest handling systems. Physical characterisation at the natural moisture content (37.55 ± 2.75% w.b.) indicated a fruit mass range of 6.51–21.31 g and mean principal dimensions of 39.30 ± 3.19 mm (length), 29.35 ± 1.41 mm (width), and 28.72 ± 1.38 mm (thickness). The calculated shape indices confirmed an ellipsoidal geometry. The static coefficient of friction was greatest on galvanised iron and lowest on stainless steel across both axial and radial orientations. The edible arillode exhibited low thermal conductivity (0.510 J/ms°C), reflecting limited heat-transfer capability. Among the predictive models evaluated, the quadratic model based on length-width-thickness (LWT) yielded the highest accuracy for mass estimation ($R^2 = 0.915$), while the criteria projected area (CPA) and oblate spheroid volume (Vosp) provided the most reliable surface-area- and volume-based predictions ($R^2 = 0.843$ and 0.838, respectively. Overall, the findings offer essential baseline data to facilitate informed machine design and optimised postharvest processing for matoa fruit.

ACKNOWLEDGEMENT

This research received financial support from the Faculty of Agricultural Technology, Universitas Brawijaya, in the framework of the BPPM funding scheme (SK: No. 40/2023 and contract number: 998/UN10.F10.06/TU/2023).

REFERENCES

Altuntaş, E., & Mahawar, M. K. (2022). Mass modelling of potato cultivars with different shape index by physical characteristics. *Journal of Food Process Engineering, 45*(10), e14126. https://doi.org/10.1111/jfpe.14126

Association of Official Analytical Chemists. (2000). *Official methods of analysis of the Association of Official Analytical Chemists*. AOAC.

Azman, P. N. M. A., Shamsudin, R., Che Man, H., & Ya'acob, M. E. (2020). Some physical properties and mass modelling of pepper berries (*Piper nigrum* L.), variety Kuching, at different maturity levels. *Processes, 8*(10), 1314. https://doi.org/10.3390/pr8101314

Barbhuiya, R. I., Nath, D., Singh, S. K., & Dwivedi, M. (2020). Mass modelling of Indian coffee plum (*Flacourtia jangomas*) fruit with its physicochemical properties. *International Journal of Fruit Science, 20*(sup3), S1110-S1133. https://doi.org/10.1080/15538362.2020.1775161

Bibwe, B., Mahawar, M. K., Jalgaonkar, K., Meena, V. S., & Kadam, D. M. (2022). Mass modelling of guava (cv. Allahabad safeda) fruit with selected dimensional attributes: Regression analysis approach. *Journal of Food Process Engineering, 45*(3), e13978. https://doi.org/10.1111/jfpe.13978

Birania, S., Attkan, A. K., Kumar, S., Kumar, N., & Singh, V. K. (2022). Mass modelling of strawberries (*Fragaria × ananassa*) based on selected physical attributes. *Journal of Food Process Engineering, 45*(5), e14023.https://doi.org/10.1111/jfpe.14023

Burley, A. L., Enright, N. J., & Mayfield, M. M. (2011). Demographic response and life history of traditional forest resource tree species in a tropical mosaic landscape in Papua New Guinea. *Forest Ecology and Management, 262*(5), 750-758. https://doi.org/10.1016/j.foreco.2011.05.008

Gade, S. R., Meghwal, M., & Prabhakar, P. K. (2020). Engineering properties of dried ash gourd (*Benincasa hispida* Cogn.) seeds: Mass modelling and its analysis. *Journal of Food Process Engineering, 43*(12), e13545.https://doi.org/10.1111/jfpe.13545

Hanafi, H., Irawan, C., Sirait, S. M., Sulistiawaty, L., & Setyawati, S. R. (2020). Toxicity test with BSLT (brine shrimp lethality test) method on methanol, ethyl acetate extract, hexane on seeds, and rind of matoa extract (*Pometia pinnata*). *Oriental Journal of Chemistry, 36*(6), 1143-1147. https://doi.org/10.13005/ojc/360618

Irawan, C., Hanafi, L. S., Rochaeni, H., & Lestari, P. S. (2017a). Comparison of total phenolic content in seed, flesh fruit and peel of *Pometia pinnata* from Indonesia. *Journal of Medicinal Plants Studies, 5*(4), 163-165. https://doi.org/10.22270/jmpas.v6i4.316

Irawan, C., Sulistiawaty, L., Rochaeni, H., & Lestari, P. S. (2017b). Evaluation of DPPH free radical scavenging activity of *Pometia pinnata* from Indonesia. *Pharma Innovation, 6*(8), 403-406. https://doi.org/10.22271/tpi.2017.v6.i8f.1111

Jacobs, M. (1962). *Pometia* (Sapindaceae), a study in variability. *Reinwardtia, 6*(2), 109-144.

Kamble, M. G., Singh, A., Mishra, V., Meghwal, M., & Prabhakar, P. K. (2021). Mass and surface modelling of green plantain banana fruit based on physical characteristics. *Computers and Electronics in Agriculture, 186*, 106194. https://doi.org/10.1016/j.compag.2021.106194

Lim, T. K. (2013). *Pometia pinnata*. In *Edible medicinal and non-medicinal plants*. Springer. https://doi.org/10.1007/978-94-007-5628-1_15

Mahawar, M. K., Bibwe, B., Jalgaonkar, K., & Ghodki, B. M. (2019). Mass modelling of kinnow mandarin based on some physical attributes. *Journal of Food Process Engineering, 42*(5), e13079. https://doi.org/10.1111/jfpe.13079

Matra, D. D., Ritonga, A. W., Natawijaya, A., Poerwanto, R., Sobir, Siregar, U. J., Widodo, W. D., & Inoue, E. (2019). Datasets for genome assembly of six underutilised Indonesian fruits. *Data in Brief, 22*, 960-963.

Murakonda, S., Patel, G., & Dwivedi, M. (2022). Characterisation of engineering properties and modelling mass and fruit fraction of wood apple (*Limonia acidissima*) fruit for post-harvest processing. *Journal of the Saudi Society of Agricultural Sciences, 21*(4), 267-277. https://doi.org/10.1016/j.jssas.2021.09.005

Panda, G., Vivek, K., & Mishra, S. (2020). Physical characterisation and mass modelling of kendu (*Diospyros melanoxylon* Roxb.) fruit. *International Journal of Fruit Science, 20*(sup3), S2005-S2017.https://doi.org/10.1080/15538362.2020.1851339

Panda, T. C., Thota, N., Dwivedi, M., Pradhan, R. C., & Seth, D. (2022). Mass modelling of engineering properties and characterisation of kadamb fruit (*Neolamarckia cadamba*): An underutilised fruit. *Journal of Food Process Engineering, 45*(11), e14160. https://doi.org/10.1111/jfpe.14160

Pathak, S. S., Pradhan, R. C., & Mishra, S. (2019). Physical characterisation and mass modelling of dried *Terminalia chebula* fruit. *Journal of Food Process Engineering, 42*(3), e12992. https://doi.org/10.1111/jfpe.12992

Pathak, S. S., Pradhan, R. C., & Mishra, S. (2020). Mass modelling of belleric myrobalan and its physical characterisation in relation to post-harvest processing and machine designing. *Journal of Food Science and Technology, 57*, 1290-1300. https://doi.org/10.1007/s13197-019-04162-1

Sahin, S., & Sumnu, S. G. (2007). *Physical properties of foods*. Springer.

Saini, P., Panghal, A., Mittal, V., & Gupta, R. (2022). Hempseed (*Cannabis sativa* L.) bulk mass modelling based on engineering properties. *Journal of Food Process Engineering, 45*(1), e13929.https://doi.org/10.1111/jfpe.13929

Sasikumar, R., Vivek, K., Chakkaravarthi, S., & Deka, S. C. (2021). Physicochemical characterisation and mass modelling of blood fruit (*Haematocarpus validus*)-An underutilised fruit of northeastern India. *International Journal of Fruit Science, 21*(1), 12-25. https://doi.org/10.1080/15538362.2020.1848752

Singh, S. S., Abdullah, S., Pradhan, R. C., & Mishra, S. (2019). Physical, chemical, textural, and thermal properties of cashew apple fruit. *Journal of Food Process Engineering, 42*(5), e13094.https://doi.org/10.1111/jfpe.13094

Singh, H., & Meghwal, M. (2020). Physical and thermal properties of various ajwain (*Trachyspermum ammi* L.) seed varieties as a function of moisture content. *Journal of Food Process Engineering, 43*(2), e13310. https://doi.org/10.1111/jfpe.13310

Sonawane, A., Pathak, S. S., & Pradhan, R. C. (2020). Physical, thermal, and mechanical properties of bael fruit. *Journal of Food Process Engineering, 43*(6), e13393. https://doi.org/10.1111/jfpe.13393

Suzuki, T., Nagata, M., Kagawa, N., Takano, S., & Nomura, J. (2021). Anti-obesity effects of matoa (*Pometia pinnata*) fruit peel powder in high-fat diet-fed rats. *Molecules, 26*(21), 6733.https://doi.org/10.3390/molecules26216733

Sweat, V. E. (1974). Experimental values of thermal conductivity of selected fruits and vegetables. *Journal of Food Science, 39*(6), 1080-1083.https://doi.org/10.1111/j.1365-2621.1974.tb07323.x

Tomar, M. S., & Pradhan, R. C. (2022). Prediction of mass-based process designing parameters of Amla fruit using different modelling techniques. *Journal of Food Process Engineering, 45*(8), e14039. https://doi.org/10.1111/jfpe.14039

Thomas, A., Pulissery, S. K., Vithu, P., & Abdullah, S. (2025). Assessment of engineering and physicochemical properties of gac fruit and predictive mass modelling for physical attributes. *Journal of Food Measurement and Characterisation, 19*, 5394-5410. https://doi.org/10.1007/s11694-025-03304-8

Vivek, K., Mishra, S., & Pradhan, R. C. (2018). Physicochemical characterisation and mass modelling of sohiong (*Prunus nepalensis* L.) fruit. *Journal of Food Measurement and Characterisation, 12*, 923-936. https://doi.org/10.1007/s11694-017-9708-x

Zulfahmi, Z., & Rosmaina, R. (2024). Phenotype variability of *Pometia pinnata* from Riau, Indonesia, based on qualitative characters. *Biodiversitas Journal of Biological Diversity, 25*(10).https://doi.org/10.13057/biodiv/d251055